MCRE-based finite element model updating: Cast3M implementation

Hugo Luiz Oliveira, François Louf, Fabrice Gatuingt

▶ **To cite this version:**

Hugo Luiz Oliveira, François Louf, Fabrice Gatuingt. MCRE-based finite element model updating: Cast3M implementation. Advances in Engineering Software, 2022, 173, pp.103220. 10.1016/j.advengsoft.2022.103220 . hal-03760608

HAL Id: hal-03760608
https://hal.science/hal-03760608

Submitted on 25 Aug 2022

HAL is a multi-disciplinary open access archive for the deposit and dissemination of scientific research documents, whether they are published or not. The documents may come from teaching and research institutions in France or abroad, or from public or private research centers.

L'archive ouverte pluridisciplinaire **HAL**, est destinée au dépôt et à la diffusion de documents scientifiques de niveau recherche, publiés ou non, émanant des établissements d'enseignement et de recherche français ou étrangers, des laboratoires publics ou privés.

MCRE-based finite element model updating: Cast3M implementation

Hugo Luiz Oliveira[a], Franois Louf[a], Fabrice Gatuingt[a]

[a] *Universit Paris-Saclay, CentraleSuplec, ENS Paris-Saclay, CNRS, LMPS - Laboratoire de Mcanique Paris-Saclay, 91190, Gif-sur-Yvette, France.*

Abstract

In structural engineering, the search for computational models capable of making realistic predictions capturing varied physical phenomena while maintaining simplicity and reliability has gained wide attention of the scientific community. Some outcomes of this effort are the finite element model updating techniques, which consists of using inverse analysis to find realistic values for the set of input parameters. The Modified Constitutive Relation Error (MCRE) has proved to be efficient for model updating in many engineering applications. The central idea of this technique is to formulate parameter identification as a well-posed optimization problem. In general, for each new MCRE application, new formulations need to be deduced and implemented. Despite the specifics of each case, there are standard features that can be abstracted and placed in a single framework. In the present work, we abstract and materialize those features into a new computational framework using Cast3M (an open-source high-level toolbox for finite elements computation). Using typical examples from structural engineering, we test the framework's efficiency and highlight its limitations. The results show that the proposed open-source code allows the identification of physical parameters for finite element models, such as stiffness, as long as physical and geometric linearity conditions remain valid. In addition, elastic inter-element interfaces can be included without significant changes. The benefits of the present study are twofold: (i) source codes are made available and can be used as learning support, in particular for newcomers, and (ii), it can be used as a starting point for new developments in the field of MCRE-based approaches.

Email address: former: oliveira@lmt.ens-cachan.fr, current: hugoitaime@alumni.usp.br (Hugo Luiz Oliveira)

Keywords: Optimization, Modified Constitutive Relation Error, Vibrating regime, Inverse analysis

1. Introduction

Modelling and simulation of structural systems are crucial activities in modern engineering and science for several reasons. For instance, at the design stage, engineers can answer particular questions about structures that have not yet come into existence. In the construction phase, these activities allow engineers to plan and execute each step to optimize costs and gain productivity. In the service phase, the same activities provide information on the instantaneous functioning of the system and thus make the decision-making process feasible. In scientific investigations, it has become common to use modelling techniques to study new phenomena in different areas of knowledge [1]. Modelling and simulation activities have gained such prominence along the last century that they are currently attributed the title of the third pillar of science, alongside theory and experimentation [2].

Among the various specialities present in modelling activities, one is of particular interest for the present work, namely, the *verification*. This speciality is dedicated to checking if the results predicted by the models correspond to observations. Ideally, the closer to reality, the more reliable the model becomes. However, in usual-life situations, accurately predicting the behaviour of structural systems is not self-evident. A new technique, called *model updating* or *parameter identification*, has emerged over the past few decades in the quest for better predictions. This technique determines which set of input parameters is most appropriate so that the corresponding model approaches reference measures in a particular scenario. The advantage is once these parameters are identified, structural predictions may perform better in scenarios other than those used to make the identification.

The literature presents various techniques capable of updating finite element models [3, 4]. These techniques may be understood according to two classes: in the *direct* techniques, the model parameters are identified relying primarily on linear algebra principles [5, 6]; on the other hand, in the *indirect* or *parametric* techniques, the model parameters are identified using consistent mechanical quantities [7, 8]. The latter is best indicated when the input parameter of interest represents a physical quantity, such as stiffness or mass. The technique employed in the present study relies on the formalism

of the Constitutive Relation Error (CRE) theory and belongs to the class of indirect methods.

The CRE formulation was initially proposed to estimate errors in finite dimension spaces [9]. Soon after, its augmented version, namely the MCRE (Modified Constitutive Relation Error), was successfully applied in finite element model updating [10]. Since then, MCRE-based techniques have been refined and expanded to different engineering fields, including, but not limited to, mechanical engineering [11], acoustics [12], automotive industry [13], aerospace structures [14, 15], topology optimization [16] and civil engineering [17, 18, 19, 20]. It is worth mentioning that inherent uncertainties can also be considered in model updating [21, 22, 23].

In modern research involving computational mechanics, the open/collaborative coding approach has increasingly gained ground in academia and industry. The joint effort of several collaborators worldwide has ensured the development of multiobjective numerical platforms such as MFEM [24], FEniCS [25], FreeFem++ [26], deal.II [27], Cast3M [28, 29], OpenFOAM [30], among others. Despite the remarkable advances in this field, open-source MCRE-based computer frameworks are still rare. The consequence is that each time a user wants to use an MCRE-based technique, a new code must be created starting from scratch.

To address this need, in the present work, we propose an abstraction of the essential elements related to usual MCRE techniques and materialize them in an open-source framework. The input data is formed by a finite set of eigenfrequencies and corresponding modal shapes. The constitutive material is assumed linear-elastic. All implementations are carried out into Cast3M, which is a general-purpose code for solving partial differential equations using the finite element method. Cast3M is distinguished from other finite element toolboxes by its intuitive lexicon and syntax, providing users with a fast learning tool. This toolbox is developed and made available by the French Atomic Energy Commission (CEA) , used in industry, research, and education [31, 32, 33, 34].

The proposed framework can be helpful to users at different levels. Newcomers to the finite element model updating field may find helpful information in the resulting sources codes once they are fully provided with considerable commented sections. They may be used in extended studies in structural analysis where engineers may be assigned to do extensions such as multiple load-cases, distinct cost functions and structural parameters. Further possibilities include using the codes as a starting point for more complex FE

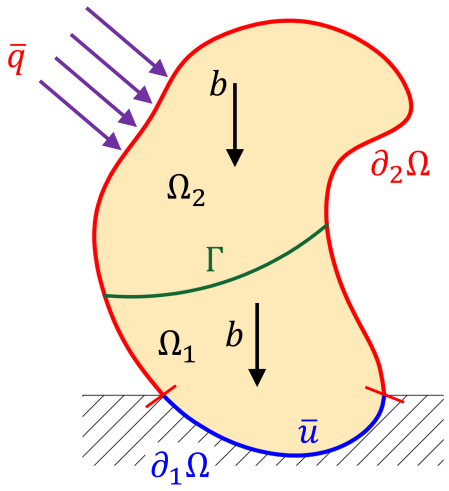

Figure 1: Solid associated to identification process. For this case, $\Omega_1 \cup \Omega_2 = \Omega$ and $\partial_1\Omega \cup \partial_2\Omega \cup \Gamma = \partial\Omega$.

model updating scenarios. Experienced users may go further, extending to the domain of structural health monitoring and even design of experiments.

2. Formulating the identification problem

2.1. The reference problem on the MCRE formalism

Let a structure be represented by $\Omega \subset \mathbb{R}^3$, with boundary, $\partial\Omega$. The structural outer surface is divided into three parts. Parts one and two are regions where the interaction between the structure and the environment occurs: kinematic constraints $\overline{\mathbf{u}}$ on a part $\partial_1\Omega$ and traction forces $\overline{\mathbf{q}}$ on $\partial_2\Omega$. The third part, Γ, is the region among sub-domains of the structure so that $\partial_1\Omega \cup \partial_2\Omega \cup \Gamma = \partial\Omega$. The situation is illustrated in Figure 1. Assuming that the entire domain follows the principles of mechanics, we are interested in identifying the structural elastic properties.

The first key aspect in formulations that follow the CRE prerogatives is separating governing equations into two sets: the *reliable* set includes all equations that must be strictly respected, and the *unreliable* set includes only the equations susceptible to be doubtful. The division of these sets is not unique, and it is up to the analyst to make the most appropriate choice for the case to be dealt with. In the present study, the following separations are made.

1. *Reliable* equations set:

   - Kinematic boundary conditions.

$$\mathbf{u}\Big|_{\partial_1\Omega} = \overline{\mathbf{u}} \tag{1}$$

   - Dynamic equilibrium.

$$\begin{aligned}\int_\Omega \rho\ddot{\mathbf{u}}\cdot\mathbf{u}^* d\Omega_i + \int_\Omega \boldsymbol{\sigma} : \boldsymbol{\varepsilon}^* d\Omega = \int_\Omega \mathbf{b}\cdot\mathbf{u}^* d\Omega_i + \\ + \int_{\partial_2\Omega} \boldsymbol{\sigma}\mathbf{n}\cdot\mathbf{u}_i^* d\partial\Omega\end{aligned} \tag{2}$$

   - Force boundary conditions.

$$\boldsymbol{\sigma}\mathbf{n}\Big|_{\partial_2\Omega} = \overline{\mathbf{q}} \tag{3}$$

2. *Unreliable* equations set:

   - Constitutive relation.

$$\mathbf{f}(\boldsymbol{\sigma}, \boldsymbol{\varepsilon}(u)) = \boldsymbol{\sigma} - \mathbb{C}(\theta) : \boldsymbol{\varepsilon} \tag{4}$$

   - Collected measures.

$$\mathbf{r}(\mathbf{u}, \tilde{\mathbf{u}}) = \mathbf{u} - \tilde{\mathbf{u}} \tag{5}$$

with $\mathbb{C}$ the Hookean stiffness operator specified by the material properties stored at θ, $\mathbf{u}$ is the displacement vector, $\boldsymbol{\sigma}$ the stress tensor, $\boldsymbol{\varepsilon}$ is the infinitesimal strain tensor, ρ the mass density, $\tilde{\mathbf{u}}$ represents the collected measures. The unreliable quantities are the constitutive relation since they may not be representative enough of the real behaviour, and the measurements because they carry errors with them. Then, the identification problem can be formulated by comparing the results predicted by the model and the experimental data. The reliable set is used to build the kinematic and static admissible spaces:

$$\mathscr{U} = \{\mathbf{u} \in H^1(\Omega) : \mathbf{u}\Big|_{\partial_1\Omega} = \overline{\mathbf{u}}\} \tag{6}$$

$$\mathscr{D} = \{\boldsymbol{\sigma} \in H^{div}(\Omega) : \text{Equation (2) holds}, \boldsymbol{\sigma}\mathbf{n}\Big|_{\partial_2\Omega} = \overline{\mathbf{q}}\} \tag{7}$$

The second key aspect in CRE-based formulations is to relate the unreliable quantities so that they are verified as well as possible. One alternative is by minimizing a functional comprising the terms considered uncertain. Here, this functional is written as follows:

$$J(\mathbf{u},\boldsymbol{\sigma},\theta) = \int_\Omega (\boldsymbol{\sigma} - \mathbb{C}(\theta)\boldsymbol{\varepsilon}) : \mathbb{C}^{-1}(\boldsymbol{\sigma} - \mathbb{C}(\theta)\boldsymbol{\varepsilon}) d\Omega + \frac{r}{2(1-r)}||\mathbf{u} - \tilde{\mathbf{u}}|| \tag{8}$$

The role played by the parameter $r \in (0,1)$ is twofold. It makes the scale order compatibility between the quantities involved and controls the importance given to the experimental measures within the functional.

Then, the parameter identification problem is written as:

$$\begin{aligned} &\text{Find } (\mathbf{u},\boldsymbol{\sigma},\theta) \text{ that minimizes } J(\mathbf{u},\boldsymbol{\sigma},\theta) \\ &\text{Such that } (\mathbf{u},\boldsymbol{\sigma}) \in \mathscr{U} \times \mathscr{D} \end{aligned} \tag{9}$$

Rather than express the entire problem at once, it is convenient to write it down into two steps as follows:

$$\min_{\mathbf{u},\boldsymbol{\sigma},\theta} J(\mathbf{u},\boldsymbol{\sigma},\theta) \Longleftrightarrow \min_{\theta} \min_{\mathbf{u},\boldsymbol{\sigma}} J(\mathbf{u},\boldsymbol{\sigma},\theta) \tag{10}$$

In practice, this choice simplifies the formulation that can be solved in two sequential steps. First, the pair of admissible fields optimally fit the fixed-parameter set θ is obtained. Then, an identification process is performed based on these admissible fields.

2.2. Obtaining mechanical admissible fields

For a given θ, the mechanical admissible fields are obtained by:

$$\begin{aligned} &\min J_1(\mathbf{u},\boldsymbol{\sigma}) + J_2(\mathbf{u}) \\ &\text{s.t. } \mathbf{u} \in \mathscr{U} \text{ and } \boldsymbol{\sigma} \in \mathscr{D} \end{aligned} \tag{11}$$

where,

$$J_1(\mathbf{u},\boldsymbol{\sigma}) = \frac{1}{2}\int_\Omega (\boldsymbol{\sigma} - \mathbb{C}\boldsymbol{\varepsilon}) : \mathbb{C}^{-1}(\boldsymbol{\sigma} - \mathbb{C}\boldsymbol{\varepsilon}) d\Omega \tag{12}$$

$$J_2(\mathbf{u}) = \frac{r}{2(1-r)}||\mathbf{u} - \tilde{\mathbf{u}}|| \tag{13}$$

The functional J_1 expresses the disparity of the stiffness properties, whereas J_2 represents a deviation from the experimental measures. The minimization of $J = J_1 + J_2$ allows verifying the unreliable equations as best as possible. Thus, all the available data are used to build the desired mechanical fields.

2.3. Identifying the optimal parameters

To each θ, it is necessary to associate a non-negative scalar that represents its quality level. Here, we use the same functional J, with the particularity that its value is calculated from the fields previously obtained (Equation (11)). In other terms:

$$F(\theta) = J(\mathbf{u}(\theta), \boldsymbol{\sigma}(\theta)) \tag{14}$$

With this definition, the lower the value of F, the better θ becomes. Then, the identification problem consists in finding the best parameters θ^* for the model by minimizing the cost function F:

$$\theta^* = \underset{\theta}{\operatorname{argmin}}\ F(\theta) \tag{15}$$

2.4. Algebraic description of the problem

The equations will be solved using the displacement-based finite element method (FEM) in this study. This choice does not represent any difficulty because the admissible stress field can be associated with an admissible displacement field, as follows:

$$\boldsymbol{\sigma}(\mathbf{v}) = \mathbb{C}\boldsymbol{\varepsilon}(\mathbf{v}) \tag{16}$$

Considering the FEM formalism, the set of displacements fields can be written as:

$$\mathbf{u}(x) = \mathrm{N}(x)\mathrm{U}, \quad \mathbf{v}(x) = \mathrm{N}(x)\mathrm{V} \tag{17}$$

where $\mathrm{N}(x)$ is the shape functions matrix, U and V are unknown nodal displacements associated to $\mathbf{u}$ and $\mathbf{v}$. Then, equation (12) can be written as:

$$J_1(\mathrm{U}, \mathrm{V}) = \frac{1}{2}(\mathrm{V} - \mathrm{U})^T \mathrm{P}(\mathrm{V} - \mathrm{U}) \tag{18}$$

where P is the stiffness matrix corresponding to the region to be identified, including interfaces considered to be elastic. Let $\tilde{\Pi}$ be a projector operator to assure the spatial correspondence between U and $\tilde{\mathrm{U}}$. Then, the experimental counterpart $||\mathbf{u} - \tilde{\mathbf{u}}||$ can be defined in a quadratic form such as:

$$J_2(\mathrm{U}, \tilde{\mathrm{U}}) = \frac{r}{2(1-r)}(\tilde{\Pi}\mathrm{U} - \tilde{\mathrm{U}})^T \mathrm{G}_u(\tilde{\Pi}\mathrm{U} - \tilde{\mathrm{U}}) \tag{19}$$

where G_u carries the stiffness terms related to the nodes where the measurements have been taken.

The identification is based on the free-vibration modes of the structure. These modes can be estimated under the assumption of sinusoidal time functions: $u(x,t) = U(x)sin(\omega t)$, $v(x,t) = V(x)sin(\omega t)$. In this cases, equation (2) becomes:

$$\mathrm{KV} - \omega^2 \mathrm{MU} = \mathrm{F} \tag{20}$$

where ω is the structural vibration frequency and F is the external excitation force. For free-vibration problems, $\mathrm{F} = 0$.

The search for admissible mechanical fields can be written as a constrained optimization problem. Introducing the Lagrange multipliers, λ, the quantity to be minimized is defined as:

$$\begin{aligned} L(\mathrm{V}, \mathrm{U}, \lambda) &= \frac{1}{2}(\mathrm{V} - \mathrm{U})^T \mathrm{P}(\mathrm{V} - \mathrm{U}) \\ &+ \frac{r}{2(1-r)}(\tilde{\Pi}\mathrm{U} - \tilde{\mathrm{U}})^T \mathrm{G}_u(\tilde{\Pi}\mathrm{U} - \tilde{\mathrm{U}}) + \lambda^T(\mathrm{KV} - \omega^2 \mathrm{MU}) \end{aligned} \tag{21}$$

For a fixed θ, the stationarity is achieved when:

$$\frac{\partial L}{\partial \mathrm{U}} = \mathrm{P}(\mathrm{U} - \mathrm{V}) + \frac{r}{(1-r)}\tilde{\Pi}^T \mathrm{G}_u(\tilde{\Pi}\mathrm{U} - \tilde{\mathrm{U}}) - \omega^2 \mathrm{M}\lambda = 0 \tag{22}$$

$$\frac{\partial L}{\partial \mathrm{V}} = \mathrm{P}(\mathrm{U} - \mathrm{V}) - \mathrm{K}\lambda \tag{23}$$

$$\frac{\partial L}{\partial \lambda} = \mathrm{KV} - \omega^2 \mathrm{MU} = 0 \tag{24}$$

These equations can be written as a linear system:

$$[\mathrm{A}]\mathrm{X} = \mathrm{Y} \tag{25}$$

where,

$$[\mathrm{A}] = \begin{bmatrix} \mathrm{P} & \frac{r}{(1-r)}\tilde{\Pi}^T \mathrm{G}_u \tilde{\Pi} & -\omega^2 \mathrm{M} \\ \mathrm{P} & 0 & -\mathrm{K} \\ -\mathrm{K} & \mathrm{K} - \omega^2 \mathrm{M} & 0 \end{bmatrix} \tag{26}$$

$$\mathrm{X} = \begin{Bmatrix} \mathrm{U} - \mathrm{V} \\ \mathrm{U} \\ \lambda \end{Bmatrix} \tag{27}$$

$$\mathrm{Y} = \begin{Bmatrix} \tilde{\Pi}^T \mathrm{G}_u \tilde{\mathrm{U}} \\ 0 \\ 0 \end{Bmatrix} \tag{28}$$

The same function was used to define both the admissible field search and the identification problem. This implies the direct access to the gradient of function (14), as follows:

$$F(\theta) = L(\mathrm{U}(\theta), \mathrm{V}(\theta), \lambda(\theta), \theta) \tag{29}$$

From the stationarity of L, it comes:

$$\frac{\partial F}{\partial \theta} = \underbrace{\frac{\partial L}{\partial \mathrm{U}}}_{=0} \frac{\partial \mathrm{U}}{\partial \theta} + \underbrace{\frac{\partial L}{\partial \mathrm{V}}}_{=0} \frac{\partial \mathrm{V}}{\partial \theta} + \underbrace{\frac{\partial L}{\partial \lambda}}_{=0} \frac{\partial \lambda}{\partial \theta} + \frac{\partial L}{\partial \theta} \tag{30}$$

$$\frac{\partial F}{\partial \theta} = \frac{\partial L}{\partial \theta} = \frac{1}{2}(\mathrm{V} - \mathrm{U})^T \frac{\partial \mathrm{P}}{\partial \theta}(\mathrm{V} - \mathrm{U}) + \lambda^T \frac{\partial \mathrm{K}}{\partial \theta}\mathrm{V} \tag{31}$$

This expression can be used to construct minimum search algorithms based on gradients.

3. Proposing the algorithm to solve the problem

3.1. Initiate model

In this step, the initial information that usually defines a finite element model should be provided, such as the geometric support of the structure, the finite element discretization (mesh) and the set of boundary conditions. It is also necessary to provide the set of measures that will be used as a reference for the identification process. Such measures are usually obtained in two ways: through previous numerical simulations of the structure in a

reference state (synthetic measurements) or direct measurements on physical structures in controlled locations, laboratories, or exposed to the environment (experimental measurements).

Distinct objective functions can be defined as a function of the reference quantities (e.g. [22, 35]). In the present work, the reference quantities are the vibration modes of the structure obtained synthetically using a dedicated FEM module (more details in Section 4).

3.2. Initiate parameter set

This step consists in choosing the initial values for the set of parameters that will be identified. Since the identification process is based on a Newton-type gradient method, the initial values influence the amount of iterations that will be necessary to obtain convergence. To improve efficiency, the analyst can benefit from previous information that one has about the structure, such as parameters obtained from preceding simulations, estimates based on empirical knowledge, statistics data and even engineering heuristics. It is worth noting that the correct value of the parameter will be provided by the algorithm at the end of the identification process. For this reason, at this stage, the analyst may privilege obtaining reasonable orders of magnitude for the initial values instead of precise estimates.

The choice of the parameters to be identified depends on the studied scenario. For example, it is known that in a given structure, zones of eventual damage are accompanied by local losses of stiffness. Thus, a correlation between these two characteristics can be established for model identification purposes. In the present study, the stiffness (linear or angular) is chosen as the parameter to be identified. This choice does not imply loss of generality since CRE theory allows much more general choices for different constitutive models [13, 36].

3.3. Calculate admissible fields

From a known set of material parameters, the corresponding admissible nodal fields $(\mathrm{U}, \mathrm{V}, \lambda)$ are determined by solving equation (25). This linear system is three times the size of the classic finite element problem. This can limit problems with a high number of degrees of freedom, particularly in three-dimensional industrial models. However, it should be noted that, for identification purposes, a reduced number of finite elements can be used efficiently. There is also the possibility of model reduction, using modal projections, among other techniques, that reduce the order of the linear system

to be solved. Here, for the sake of simplicity in coding, it is used the full version of equation (25).

3.4. Calculate global MCRE

The global MCRE is obtained from equations (18) and (19) such as:

$$J(\mathrm{U}, \mathrm{V}, \tilde{\mathrm{U}}) = J_1(\mathrm{U}, \mathrm{V}) + J_2(\mathrm{U}, \tilde{\mathrm{U}}) \tag{32}$$

The result is a scalar quantity necessary for the convergence test.

3.5. Convergence criterion

There are two convergence tests immediately available. The first one assumes convergence is achieved whenever:

$$J(\mathrm{U}, \mathrm{V}, \tilde{\mathrm{U}}) < \xi_1 \tag{33}$$

The second assumes convergence is achieved when no improvement is observed for a limited number of consecutive iterations (5 in our tests), that is:

$$||J_i(\mathrm{U}, \mathrm{V}, \tilde{\mathrm{U}}) - J_{i-1}(\mathrm{U}, \mathrm{V}, \tilde{\mathrm{U}})|| < \xi_2 \tag{34}$$

where ξ_1 and ξ_2 are small positive values. The most appropriate choice may depend on the case handled by the analyst.

3.6. Calculate CRE field

In practical applications, for the sake of efficiency, it may be beneficial not to update all stiffness parameters simultaneously. When the region to be identified is not known *a priori*, a simple strategy can be drawn based on equation (18). It carries the information about how well the material parameters of the model correspond to reality. So, the structure can be divided into sub-regions, and the quantity of J_1 for each of them can be obtained. Using relative comparisons, regions with higher modelling errors will indicate higher values of J_1, and therefore they should have their parameters updated first. Suppose that n sub-regions were defined for the calculation of J_1. In this case, the indicator β is written as:

$$\beta_j = \frac{J_1(\mathrm{U}, \mathrm{V})_j}{\sum_{j=1}^{n} J(\mathrm{U}, \mathrm{V})_j} \tag{35}$$

The higher the value of this indicator, the greater the participation of the corresponding region in the global error, and consequently, it should receive priority for updating. This strategy can be automated to work adaptively.

3.7. Update material parameters

The regions selected in the previous step will have their material parameters updated. From a set of known values θ_i, one attempts to determine an improved set θ_{i+1}. There are different ways available for this purpose, such as Newton or BFGS method. Here, we use a simple steepest gradient, such that;

$$\text{Compute } \nabla\theta \text{ from equation (31)} \tag{36}$$

$$\text{Compute } s \text{ solving } \min_s F(\theta - s\nabla\theta) \tag{37}$$

$$\Delta\theta_{i+1} = -s\nabla\theta \tag{38}$$

$$\theta_{i+1} = \theta_i + \Delta\theta_{i+1} \tag{39}$$

The flowchart in Figure 2 shows how these tasks are arranged. This framework can be implemented using any FEM purpose language. Here, Gibiane version 2020 was chosen for all applications [29].

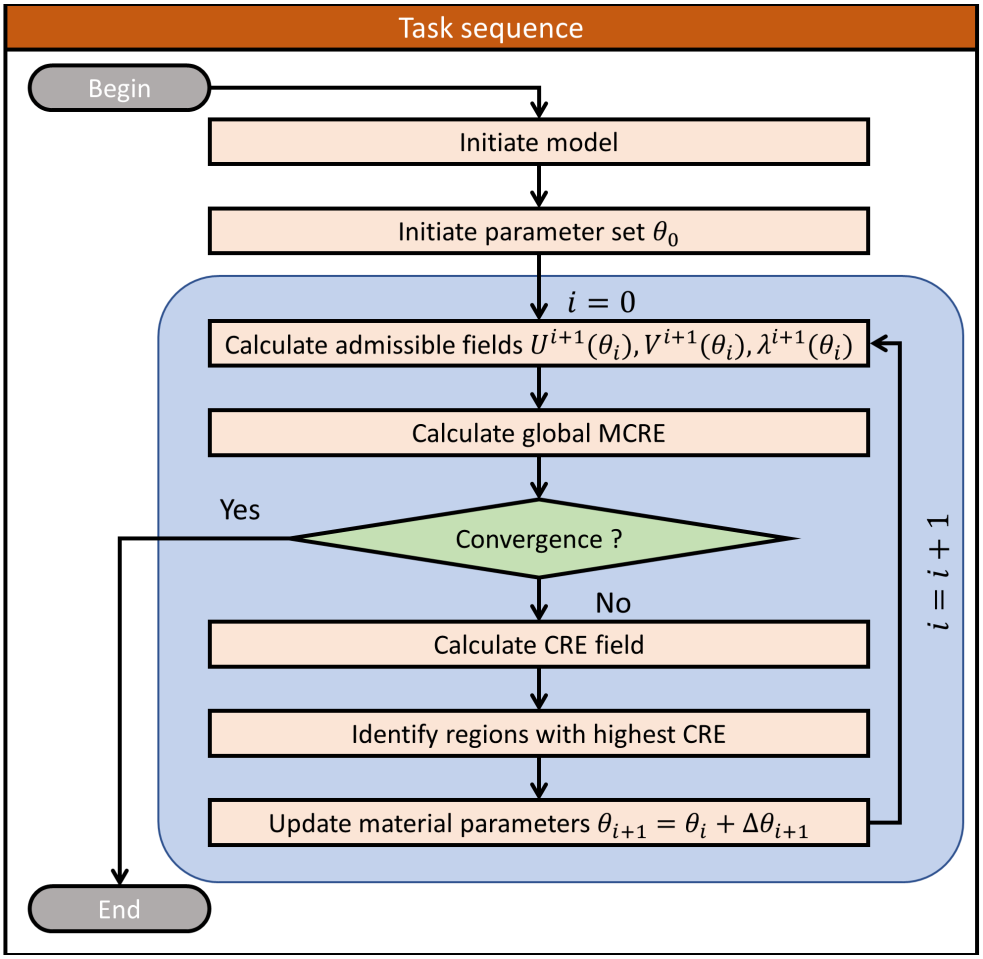

Figure 2: Task sequence for solving the identification problem.

4. Cast3M implementation

Four modules were designed to facilitate the application and expansion of the proposed framework. These modules, specified through independent Gibiane files, contain information related to geometry, models and materials, reference measures, and model updating core processing. For each application, these files must be filled in with the correspondent information and then executed separately in order to produce their outputs. The communication between the different modules is done via writing and reading commands (SAUV, REST), as shown in Figure 3.

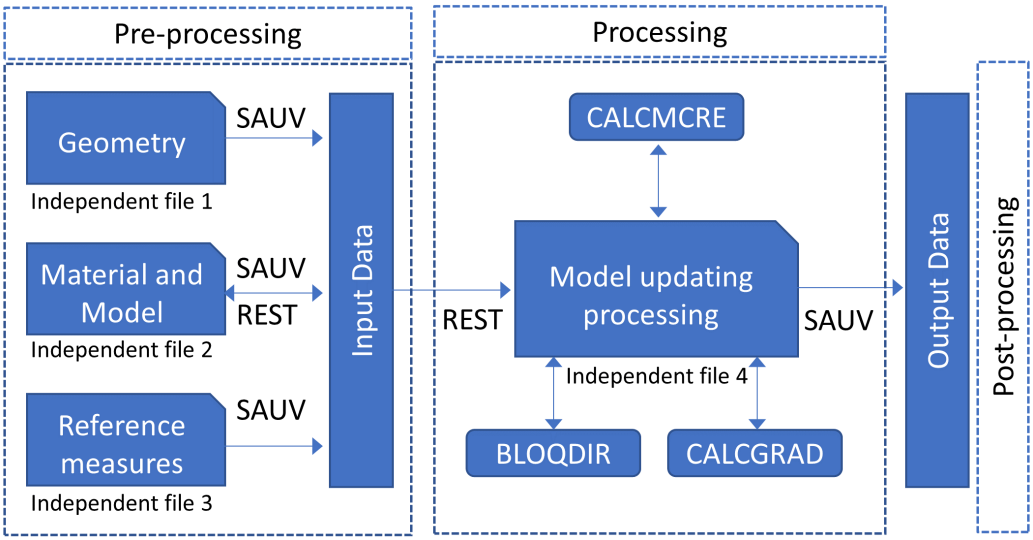

Figure 3: Communication diagram.

4.1. Geometry

In this module, all information about the geometry of the finite element model to be updated must be provided. All the options available for reticular, planar and volumic elements remain valid.

```
*****************************************
* Defining the spatial dimension and the
* the root finite elements library
'OPTI' 'DIME' 3 'ELEM' 'CUB8' ;
*****************************************
* Number of elements allocated to each pillar
NEL = 6;
* Geometric nodes
P1 = 0.0000  0.0000  0.0000;
P2 = 0.0000  0.0000  3.0000;
P3 = 0.0000  0.0000  6.0000;
P4 = 0.0000  0.0000  9.0000;
* Creating pillars
L1 = 'DROI' NEL P1 P2;
L2 = 'DROI' NEL P2 P3;
L3 = 'DROI' NEL P3 P4;
* Creating the set of pillars to be updated
PI_UPD = L1 'ET' L2;
* Pillars not to be updated
PI_N_UPD = L3;
*
*****************************************
```

Figure 4: Illustration: three-pillar geometry definition.

The regions of the model that will be updated and those that will not must be adequately identified. As an illustration, consider a structure consisting of three pillars, three metres long each, aligned along the z-direction. Suppose we want to update only two of the three pillars (L1, L2). In this case, Figure 4 shows how the geometry file would be filled. Dedicated procedures and other external subroutines calls can be used inside this module for more complex geometries.

4.2. Material and Model

In this module, it is necessary to inform the constitutive models and the kinematic hypotheses involved (beam, plate, shell, etc.), as well as the necessary characteristics of each one. As previously stated, only geometrically linear elastic models should be considered.

As in the case of geometry, each region that will be updated, and those that will not, must be adequately identified. In the example of the three pillars, the proper way to fill out this file is the way indicated in Figure 5.

```
*******************************************
*Material properties
MOD1 = 3.2E10;
PES1 = 2500;
COE1 = 0.2;
*Cross section properties
PILSEC = 0.16;
OY = 1. 0. 0.;
IN_OY = 2.1E-3;
IN_OZ = 2.1E-3;
IN_TOR= 4.0E-3;
* Model and material instances to be updated
MOD1 = 'MODEL' PI_UPD 'MECANIQUE'
   'ELASTIQUE' 'POUT';
MAT1 = 'MATE' MOD1 'YOUN' MOD1 'NU' COE1
       'RHO' PES1;
CAR1 = 'CARA' MOD1 'SECT' PILSEC 'INRY' IN_OY
       'INRZ' IN_OZ 'TORS' IN_TOR 'VECT' OY;
MAT1 = MAT1 'ET' CAR1;
* Model and material instances unchanged
MOD2 = 'MODEL' PI_N_UPD 'MECANIQUE'
       'ELASTIQUE' 'POUT';
MAT2 = 'MATE' MOD2 'YOUN' MOD1 'NU' COE1
       'RHO' PES1;
CAR2 = 'CARA' MOD2 'SECT' PILSEC 'INRY' IN_OY
       'INRZ' IN_OZ 'TORS' IN_TOR 'VECT' OY;
MAT2 = MAT2 'ET' CAR2;
*
*******************************************
```

Figure 5: Illustration: three pillar model and material definition.

4.3. Reference Measures

In this module, information on the reference measures (frequencies and mode shapes) should be provided. They can be obtained from experiments or

other numerical simulations. It is worth mentioning that the analyst should be careful about the boundary conditions because they directly influence the physical parameter to be identified, in particular within a low-frequency spectrum.

In the case of the pillar model, assuming a sinusoidal shape for the first vibration mode and a frequency of $0.83Hz$, Figure 6 illustrates how the measures could be manually set up. The reference measures are always stored in TABLE format, even if it contains only one input.

```
*******************************************
*Reference modes
*
STR = L1 'ET' L2 'ET' L3;
C1  = 'COOR' STR 3;
C2  = 'SIN ' ((C1/9.)*(180./3.14));
U1  = 'CHAN' C2 'COMP' 'UX';
U2  = 0.*('CHAN' C2 'COMP' 'UY');
U3  = 0.*('CHAN' C2 'COMP' 'UZ');
U   = U1 'ET' U2 'ET' U3;
*
FREQREF = TABLE;
MODEREF = TABLE;
*
FREQREF . 1 = 0.83 ;
MODEREF . 1 = U;
*
RES1 = 'TABLE';
RES1 . 'NB_OF_REFERENCE_MODES' = 1;
RES1 . 'REFERENCE_FREQUENCIES' = FREQREF;
RES1 . 'REFERENCE_MODE'        = MODEREF;
*
*******************************************
```

Figure 6: Illustration: defining the first reference mode and frequency for the three pillar model.

In the case the reference modes come from experiments, the data must be organized in the form CHPOINT before being stored in the reference table.

4.4. Model Updating Processing

The three previous modules serve to organize the information in a structured manner so that the processing module can be carried out appropriately. The present module corresponds to the implementation of the tasks shown in Figure 2, which requires the use of two three auxiliary procedures, which are described below.

4.4.1. Procedure: CALCMCRE

This procedure takes as input the reference measures, geometry, model and material properties and calculates the admissible nodal fields (Equation (25)).

4.4.2. Procedure: CALCGRAD

This procedure takes the admissible fields and current material properties as input and provides the calculation of the gradient of the quantities to be updated (Equation (31)).

4.4.3. Procedure: BLOQDIR

This procedure is used to impose the boundary conditions on the admissible fields before the linear system solution in CALCMCRE. Here we have opted for the penalization method so that the standard algorithm for solving systems of equations, available in Cast3M, can be used directly. However, other ways, such as Lagrange multipliers, are possible. In this case, attention should be paid to possible conflicts in managing internal software indexes.

5. Numerical examples

In this Section, typical examples from the engineering field illustrate how the framework discussed in the previous sections is helpful. The corresponding source codes were implemented in Gibiane language (Version 2020) and can be found on the publisher's website.

5.1. Revealing poorly modelled regions

One of the valuable features of the proposed framework is the ability to indicate poorly modelled regions, regions in which the values of material properties (such as stiffness) are far from their reference values. To illustrate this ability, we use the Mottershead beam [3] with the following reference parameters: $L = 0.7m$, $EI = 4560Nm^2$, $\rho = 2860kg/m^3$, $k_r = 1.0 \times 10^5 Nm/rad$

(angular stiffness) and $k_t = 4.0 \times 10^7 N/m$ (translational stiffness). The discrete model was divided into eleven regions, being ten elementary regions, each containing three finite elements, and an interface region where the boundary conditions are specified. The scenario is depicted in Figure 7.

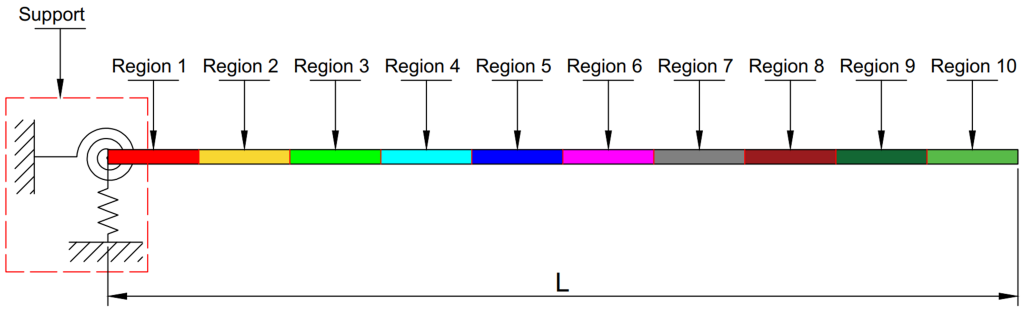

Figure 7: Beam geometry and boundary conditions.

The test consists in introducing a defect in region seven by reducing the Young modulus to 50%. Then, we solve equation (25) for obtaining the corresponding admissible fields used to calculate the indicator index from equation (35) for each region of the beam. Then, we solve equation (25) for obtaining the corresponding admissible fields used to calculate the indicator index from equation (35) for each region of the beam. The result is shown in Figure 8.

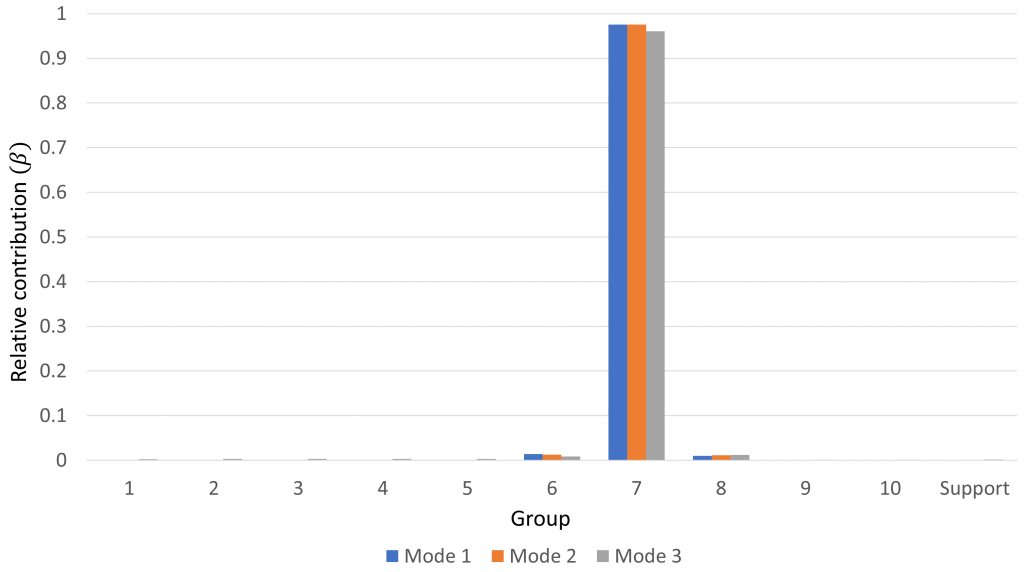

Figure 8: Contribution of each structural region to compose the global CRE, considering the first three mode shapes. Compared to the other regions, the prominence of the contribution shown by region seven indicates that it is poorly modelled.

Comparing the relative contribution of each region, it is possible to notice that region 7 has a β index around 0.97 for the first three modes of vibration. This information can be used to produce a more efficient identification algorithm because instead of identifying parameters of the structure as a whole, this procedure can be carried out by sub-zones, following the highest β values until global convergence is achieved.

Then, the test is repeated twice more. Firstly, the damage (50% of stiffness) is included in region 3. Then, the damage is additionally present in regions 1, 5 and 9. Figures 9 and 10 show the new distribution of β for each case. We observe that the prominence in the relative contribution corresponds precisely where the defects are. However, note that the β levels do not remain the same for the different vibration modes. For instance, according to Figure 9, region 3 affects the first vibration mode much more than region 7. This information can be useful in designing real-life experiments, as it is possible to know in advance which mode of vibration must be mobilized to update the parameters of a particular region of the structure.

These tests show that the framework has a capacity to distinguish between well and poorly modelled zones in the constitutive relation error sense.

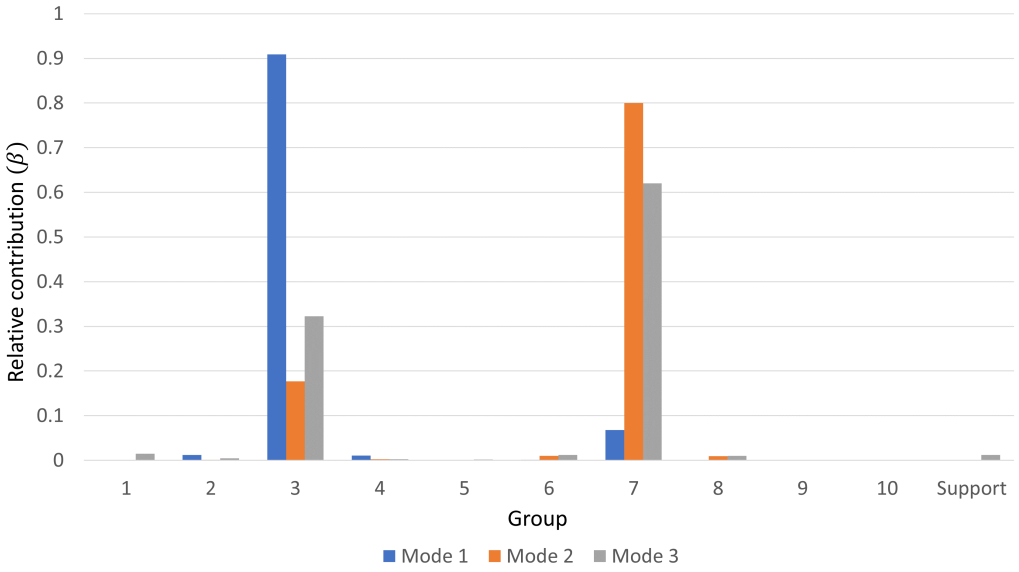

Figure 9: Contribution of each region of the structure to compose the global CRE, considering the first three modes. The prominence showed by regions 3, and 7 indicate they are being poorly modelled compared to the others.

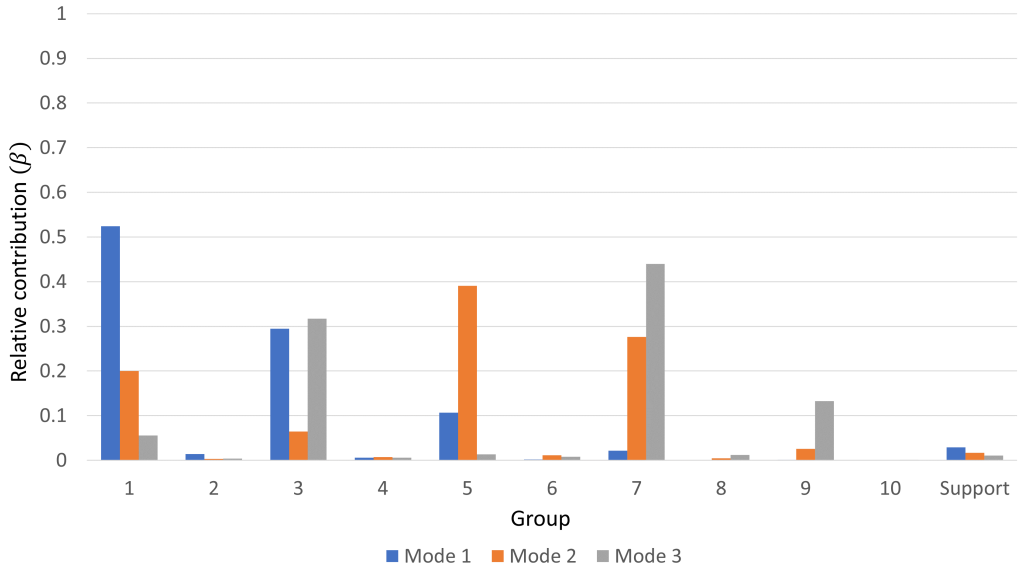

Figure 10: Contribution of each region of the structure to compose the global CRE, considering the first three modes. The prominence is shown by regions 1, 3, 5, 7 and 9; corresponding to the zones where damage is located.

5.2. Uni-parametric identification (beam-plate structure)

The typology of the present application is recurrent in the literature, being very useful in studying structural elements and their connections [18]. Here, we are interested in identifying Young's modulus of the slabs in a three-storey building structure. Each slab is $4\,m \times 4\,m$ area and $0.15\,m$ thickness. The cross-section is $40\,cm \times 40\,cm$ for pillars and $20\,cm \times 50\,cm$ for the beams. The material properties of pillars and beams are: Young modulus $32\,GPa$, Poisson's ratio 0.2 and mass density $2500\,kg/m^3$. The material properties are assumed the same for all slabs, making the problem a uni-parametric identification. The inter-floor distance is $3\,m$. In Figure 11, it is shown a three-dimensional view of the building and also the finite element model used.

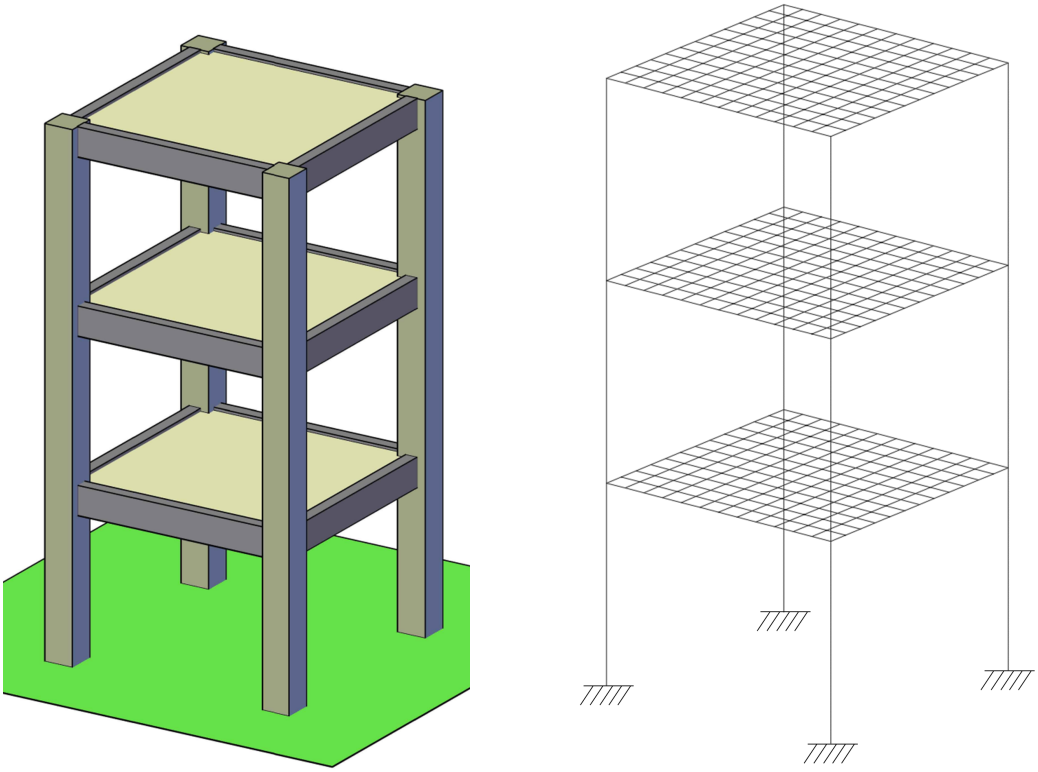

(a) (b)

Figure 11: Building structure. (a) Three-dimensional representation. (b) Structural model composed of beams and plates.

The first three vibration modes used as reference are shown in Figure 12. They were obtained via forward analysis, assuming that slabs have the same material parameters as the columns and beams.

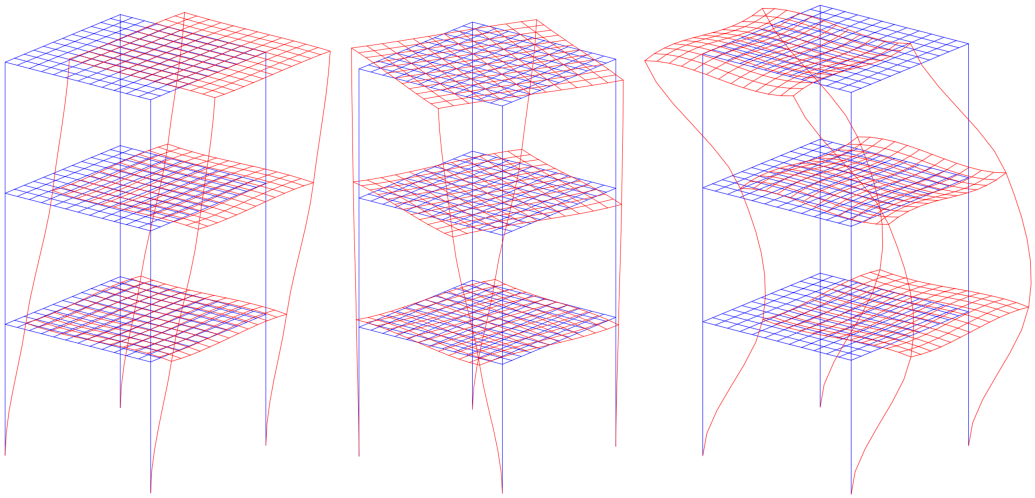

(a) (b) (c)

Figure 12: Building reference vibration modes: (a) Mode I, 4.34 Hz, (b) Mode II, 6.31 Hz, (c) Mode III, 14.24 Hz.

Setting the initial parameter value (θ_0) to 3.2 GPa, it is possible to follow the framework from Figure 2. The evolution of the MCRE as a function of θ/θ_{ref} can be seen in Figure 13. The logarithmic scale used to express the MCRE value shows the rapid convergence in the vicinity of the reference value. When the algorithm finds the appropriate parameter value, the MCRE value tends to zero. This characteristic is preserved in cases such the present, where the reference modes are obtained numerically. In real-world problems, the zero value is rarely attainable due to the numerous sources of uncertainties associated with the measurements taken, the models employed and their respective solution techniques. Despite this, the trend of rapid local decrease in the MCRE values remains a good indicator for finding values of unknown parameters (θ).

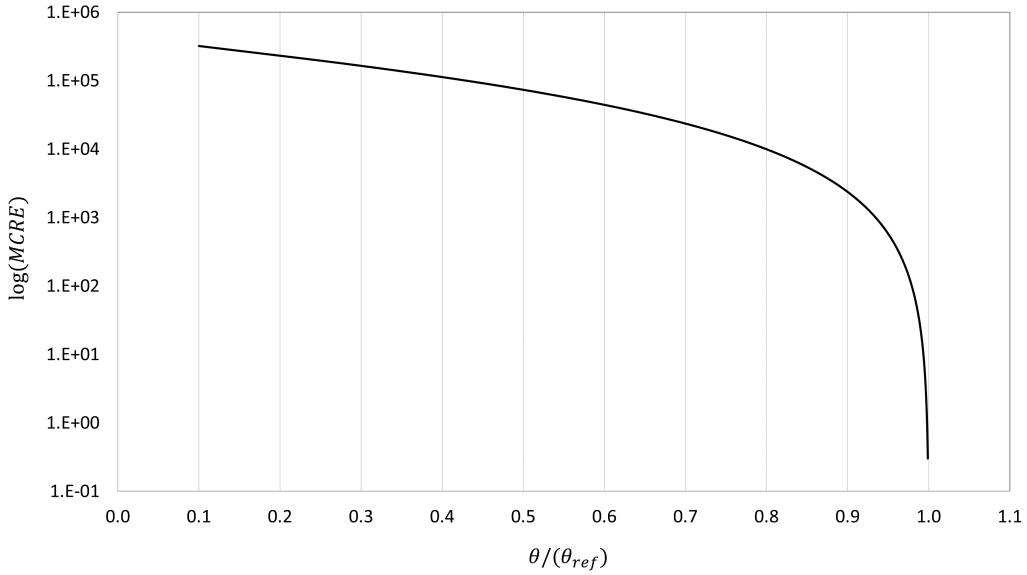

Figure 13: Identification of slabs stiffness. The searched parameter is identified when the MCRE value tends to zero.

This test permits observing that, in the absence of noise, the framework can find the correct value of the parameter sought even when the initial estimate is far from the reference. This property is desirable in numerical applications, as it helps to maintain good stability and convergence characteristics.

5.3. Multi-parametric identification (shell structure)

In this last application, one is interested in the behaviour of the framework when several parameters must be identified at the same time. For this end, it is proposed the identification of multiple stiffness parameters of a cooling tower. For sake of simplicity, only the shell structure is considered (adapted from [37]). Similarly to the first application, the tower is subdivided into five regions with their own material and geometric characteristics. The schematic scenario is illustrated in Figure 14. The regions high are $H_1 = 14.43\,m$, $H_2 = 14.43\,m$, $H_3 = 157.50\,m$, $H_4 = 43.80\,m$ and $H_5 = 6.80\,m$. The thickness of each region is $t_1 = 1.50\,m$, $t_2 = 1.50\,m$, $t_3 = 1.50\,m$, $t_4 = 1.40\,m$ and $t_5 = 1.0\,m$. The diameters are $\phi_1 = 176.56\,m$, $\phi_2 = 165.80\,m$, $\phi_3 = 156.04\,m$, $\phi_4 = 107.30\,m$, $\phi_5 = 113.26\,m$ and $\phi_6 = 114.18\,m$. The base is prevented from moving in each of the three Cartesian directions.

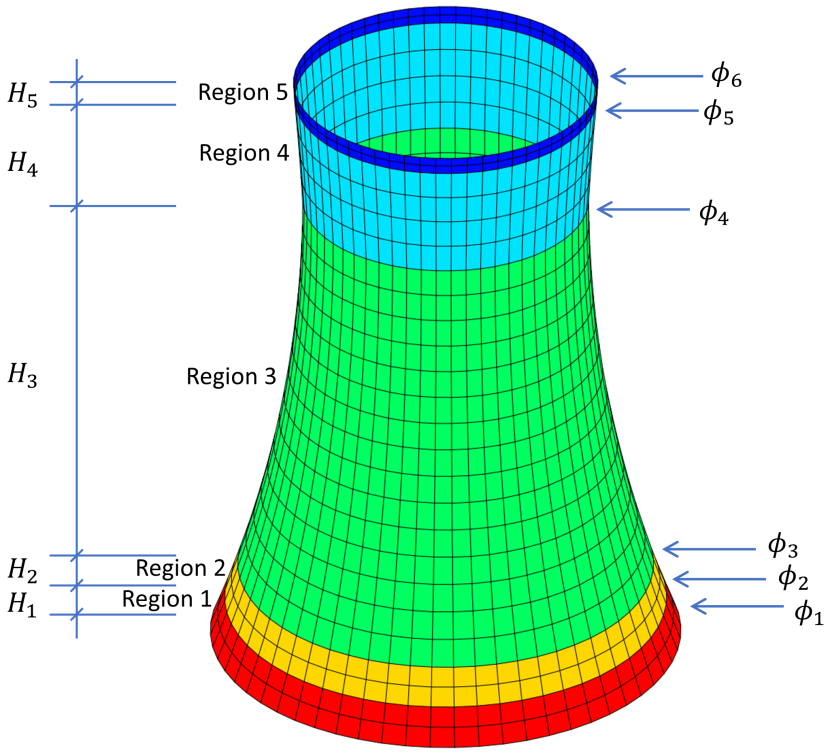

Figure 14: Cooling tower model (adapted from [37]).

The first three vibration modes used as a reference can be seen in Figure 15. They were obtained through forward analysis using the following parameters, which are the same among all regions: Young modulus $32\,GPa$, Poisson's ratio 0.2 and mass density $2500\,kg/m^3$.

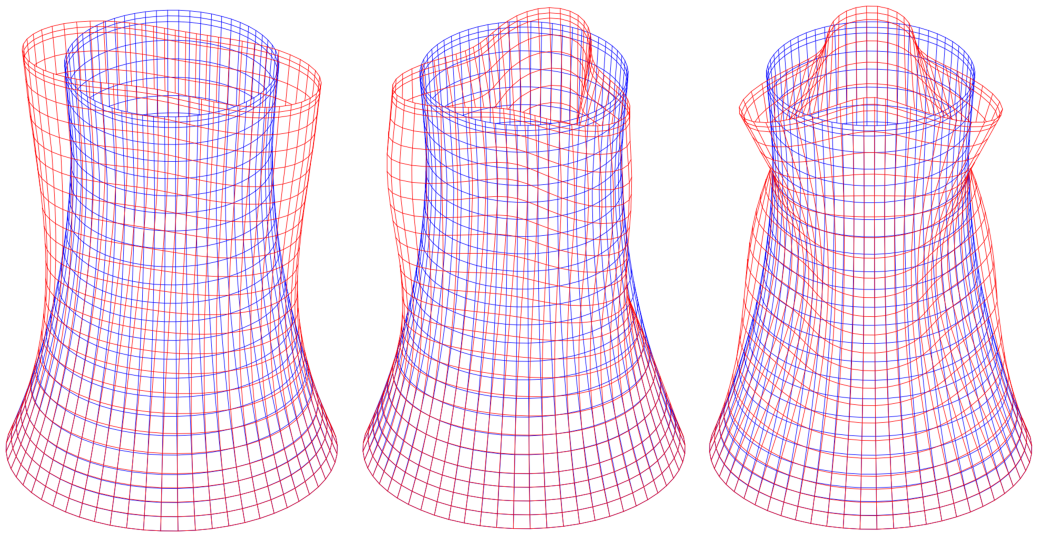

(a) (b) (c)

Figure 15: Cooling tower reference vibration modes: (a) Mode I, $0.90\,Hz$, (b) Mode II, $0.95\,Hz$, (c) Mode III, $1.20\,Hz$.

The parameters chosen to be identified are the Young moduli of regions 2, 3, 4 and 5. The initial values setting are: $\theta_0 = \{16, 48, 16, 16\}\,GPa$. The convergence history for the four chosen parameters can be seen in Figure 16. It is possible to notice that the convergence rate for each parameter is not the same. As the input data does not suffer any type of noise, all parameters could be identified correctly. In real-world scenarios, parameters with a low convergence rate can be drastically affected by uncertainties, and therefore filtering techniques may be helpful and can be coupled in the framework without major changes.

The value of the parameters is calculated based on the gradient method. However, the convergence curve shows that second-order algorithms such as BFGS can improve performance, which can also be implemented in the present framework.

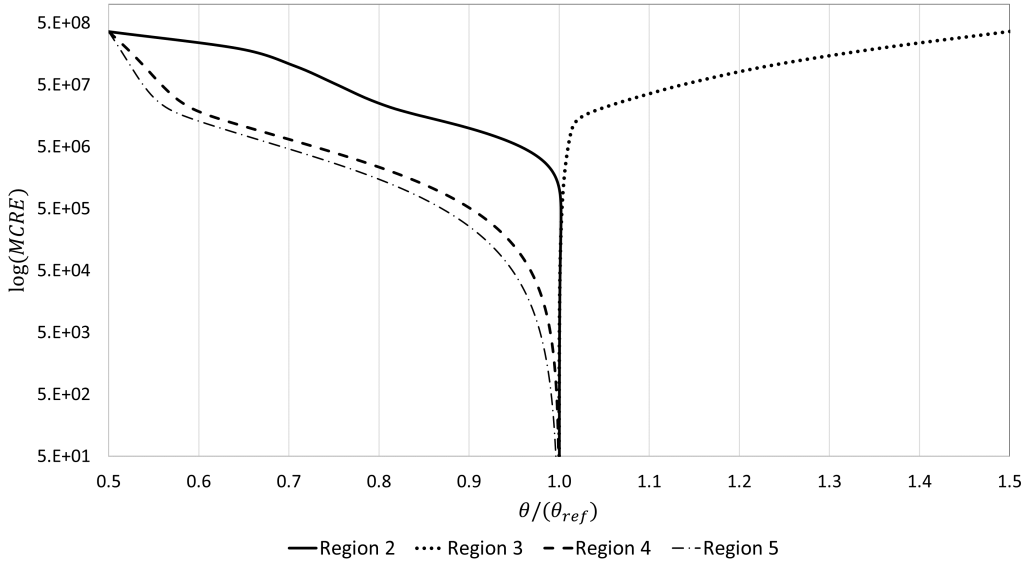

Figure 16: Cooling tower stiffness identification. The searched parameter corresponding to each region is identified when the MCRE value tends to zero.

What is pertinent to note from this test is that the framework, in the absence of measurement noise, is able to identify target parameters with high precision, even if they have low convergence rates or have vague initial estimates.

Concluding remarks

The present study dealt with the finite element model identification technique based on Modified Constitutive Relation Error. This technique was used to design an open-source framework that identifies physical parameters, such as stiffness, in typical structural engineering situations. The framework was tested in representative scenarios of engineering practice in the absence of noise, and in all cases studied, it was able to identify the parameters sought accurately.

The results presented in this paper are far from exhaustive, and we do not have this intention either. We prefer to limit ourselves to proposing to the community of scientists and engineers an open-source code that can be used for educational and research purposes. Newcomers to the finite element model updating field can use the proposed framework to gain insights into the

domain. Also, they can use the provided codes as starting points for other specific activities. Researchers may use the framework either to change it according to their needs or as a black-box subroutine for complementary codes.

The framework was developed in a modular way and is, therefore, able to accommodate new functions and behaviours without significant changes. An immediate extension would be the insertion of the effects of uncertainties or physical nonlinearities. It is also possible to extend the present framework to contemplate the cases of experiment design, in which the position and quantity of sensors can be obtained even before starting the tests.

We believe that the present framework can be helpful to the model updating community, both for a deeper study of the formulation properties and for its expansion.

Acknowledgements

Within the SINAPS@ project, this work benefited from French state funding managed by the National Research Agency under program RNSR Future Investments bearing reference no. ANR11RSNR002204. The research reported in this paper has been supported in part by the SEISM Paris Saclay Research Institute.

[1] M. Calder, C. Craig, D. Culley, R. de Cani, C. A. Donnelly, R. Douglas, B. Edmonds, J. Gascoigne, N. Gilbert, C. Hargrove, et al., Computational modelling for decision-making: where, why, what, who and how, Royal Society open science 5 (2018) 172096.

[2] M. Farge, Numerical experimentation: A third way to study nature, in: Frontiers of Computational Science, Springer, 2007, pp. 15–30.

[3] M. Friswell, J. E. Mottershead, Finite element model updating in structural dynamics, volume 38, Springer Science & Business Media Dordrecht, 1995.

[4] B. A. Zárate, J. M. Caicedo, Finite element model updating: Multiple alternatives, Engineering Structures 30 (2008) 3724–3730.

[5] Y. Yang, Y. Chen, A new direct method for updating structural models based on measured modal data, Engineering Structures 31 (2009) 32–42.

[6] M. Girardi, C. Padovani, D. Pellegrini, M. Porcelli, L. Robol, Finite element model updating for structural applications, Journal of Computational and Applied Mathematics 370 (2020) 112675.

[7] J. M. W. Brownjohn, P. Moyo, P. Omenzetter, Y. Lu, Assessment of highway bridge upgrading by dynamic testing and finite-element model updating, Journal of Bridge Engineering 8 (2003) 162–172.

[8] J. E. Mottershead, M. Link, M. I. Friswell, The sensitivity method in finite element model updating: A tutorial, Mechanical systems and signal processing 25 (2011) 2275–2296.

[9] P. Ladeveze, D. Leguillon, Error estimate procedure in the finite element method and applications, SIAM Journal on Numerical Analysis 20 (1983) 485–509.

[10] P. Ladevèze, D. Nedjar, M. Reynier, Updating of finite element models using vibration tests, AIAA journal 32 (1994) 1485–1491.

[11] P. Ladevèze, L. Chamoin, The constitutive relation error method: A general verification tool, in: Verifying Calculations-Forty Years On, Springer, 2016, pp. 59–94.

[12] V. Decouvreur, P. Bouillard, A. Deraemaeker, P. Ladevèze, Updating 2d acoustic models with the constitutive relation error method, Journal of sound and vibration 278 (2004) 773–787.

[13] V. Decouvreur, P. Ladevèze, P. Bouillard, Updating 3d acoustic models with the constitutive relation error method: A two-stage approach for absorbing material characterization, Journal of sound and vibration 310 (2008) 985–997.

[14] D. Barthe, A. Deraemaeker, P. Ladeveze, S. L. Loch, Validation and updating of industrial models based on the constitutive relation error, AIAA journal 42 (2004) 1427–1434.

[15] P.-E. Charbonnel, P. Ladevèze, F. Louf, C. Le Noach, A robust cre-based approach for model updating using in situ measurements, Computers & Structures 129 (2013) 63–73.

[16] C. Sanders, J. Norato, T. Walsh, W. Aquino, An error-in-constitutive equations strategy for topology optimization for frequency-domain dynamics, Computer Methods in Applied Mechanics and Engineering 372 (2020) 113330.

[17] Z. Djatouti, J. Waeytens, L. Chamoin, P. Chatellier, Coupling a goal-oriented inverse method and proper generalized decomposition for fast and robust prediction of quantities of interest in building thermal problems, in: Building Simulation, volume 13, Springer, 2020, pp. 709–727.

[18] X. Hu, E. Chodora, S. Prabhu, S. Atamturktur, Extended constitutive relation error-based approach: The role of mass in damage detection, Structural Control and Health Monitoring 26 (2019) e2318.

[19] H. Oliveira, F. Louf, E. Hervé-Secourgeon, F. Gatuingt, Wall-slab joint parameter identification of a reinforced concrete structure using possibly corrupted modal data, International Journal for Numerical and Analytical Methods in Geomechanics 44 (2020) 19–39.

[20] H. L. Oliveira, E. D. Leonel, Constitutive relation error formalism applied to the solution of inverse problems using the bem, Engineering Analysis with Boundary Elements 108 (2019) 30–40.

[21] S.-S. Jin, Y.-S. Park, S. Kim, Y.-H. Park, Model updating based on mixed-integer nonlinear programming under model-form uncertainty in finite element model, Engineering with Computers (2020) 1–27.

[22] M. Diaz, P.-E. Charbonnel, L. Chamoin, Robust energy-based model updating framework for random processes in dynamics: application to shaking-table experiments, Computers and Structures (2022) in press.

[23] H. L. Oliveira, F. Louf, F. Gatuingt, Numerical study based on the constitutive relation error for identifying semi-rigid joint parameters between planar structural elements, Engineering Structures (2021) 112015.

[24] R. Anderson, J. Andrej, A. Barker, J. Bramwell, J.-S. Camier, J. Cerveny, V. Dobrev, Y. Dudouit, A. Fisher, T. Kolev, et al., Mfem: a modular finite element methods library, arXiv preprint arXiv:1911.09220 (2019).

[25] M. Alnæs, J. Blechta, J. Hake, A. Johansson, B. Kehlet, A. Logg, C. Richardson, J. Ring, M. E. Rognes, G. N. Wells, The fenics project version 1.5, Archive of Numerical Software 3 (2015).

[26] F. Hecht, New development in freefem++, Journal of numerical mathematics 20 (2012) 251–266.

[27] D. Arndt, W. Bangerth, B. Blais, M. Fehling, R. Gassmöller, T. Heister, L. Heltai, U. Köcher, M. Kronbichler, M. Maier, et al., The deal. ii library, version 9.3, Journal of Numerical Mathematics 29 (2021) 171–186.

[28] P. Verpeaux, A. Millard, T. Charras, A. Combescure, A modern approach of large computer codes for structural analysis, IASMiRT (1989).

[29] CEA, Cast3m website, http://www-cast3m.cea.fr/index.php, 2020.

[30] Openfoam, 2021. URL: `https://www.openfoam.com/`.

[31] C. Guerin, C. Cappelaere, M. Ton-That, Cast3m modelling of dynamic experiments on pwr high burn-up fuel rods equivalent fuel rod modelling approach validation, Mechanics & Industry 20 (2019) 808.

[32] B. Bary, C. Bourcier, T. Helfer, Analytical and 3d numerical analysis of the thermoviscoelastic behavior of concrete-like materials including interfaces, Advances in Engineering Software 112 (2017) 16–30.

[33] B. Richard, G. Rastiello, C. Giry, F. Riccardi, R. Paredes, E. Zafati, S. Kakarla, C. Lejouad, Castlab: an object-oriented finite element toolbox within the matlab environment for educational and research purposes in computational solid mechanics, Advances in Engineering Software 128 (2019) 136–151.

[34] L. Chougrani, J.-P. Pernot, P. Véron, S. Abed, Parts internal structure definition using non-uniform patterned lattice optimization for mass reduction in additive manufacturing, Engineering with Computers 35 (2019) 277–289.

[35] B. Marchand, L. Chamoin, C. Rey, Parameter identification and model updating in the context of nonlinear mechanical behaviors using a unified

formulation of the modified constitutive relation error concept, Computer Methods in Applied Mechanics and Engineering 345 (2019) 1094–1113. doi:https://doi.org/10.1016/j.cma.2018.09.008.

[36] C. Gouttebroze, F. Louf, L. Champaney, Multiple model updating using the finite element method over a polynomial algebra, Inverse problems 26 (2010) 065001.

[37] Q.-Q. Yu, X.-L. Gu, Y. Li, F. Lin, Collapse mechanism of reinforced concrete superlarge cooling towers subjected to strong winds, Journal of Performance of Constructed Facilities 31 (2017) 04017101.